Aalborg Universitet

A Hybrid Islanding Detection Technique Using Average Rate of Voltage Change and Real Power Shift

Mahat, Pukar; Chen, Zhe; Bak-Jensen, Birgitte

Link to publication from Aalborg University

A Hybrid Islanding Detection Technique Using Average Rate of Voltage Change and Real Power Shift

Pukar Mahat, Zhe Chen and Birgitte Bak-Jensen

Abstract— The mainly used islanding detection techniques may be classified as active and passive techniques. Passive techniques don't perturb the system but they have larger non-detection zones, whereas active techniques have smaller non-detection zones but they perturb the system. In this paper, a new hybrid technique is proposed to solve this problem. An average rate of voltage change (passive technique) has been used to initiate a real power shift (active technique), which changes the real power of distributed generation (DG), when the passive technique cannot have a clear discrimination between islanding and other events in the system. Simulation results show that the proposed method is effective in detecting islanding of distribution systems with DGs.

Index Terms-- Distributed generation, islanding detection, real power shift, voltage change.

I. INTRODUCTION

There is a renewed interest in the distributed generation mainly due to the environmental concern and electricity market liberalization. Many utilities around the world already have a significant penetration of DG in their systems. But there are many issues to be resolved before DG becomes an integral part of the utilities around the world. One of the main issues with DG is islanding. Islanding is a situation in which a distribution system becomes electrically isolated from the remainder of the power system, due to a fault upstream or any other disturbance, and yet continues to be energized by the DG connected to it. Current practice is that almost all utilities require the DG to be disconnected from the grid as soon as possible in case of islanding. IEEE 929-1988 standard [1] requires the disconnection of DG once it is islanded and IEEE 1547-2003 standard [2] stipulates a maximum delay of 2 seconds for detection of an unintentional island and all DGs ceasing to energize the distribution system. Hence, it is essential to detect the islanding both quickly and accurately.

Many techniques have been proposed for detecting islanding [3]-[21]. Recent developments in islanding detection are reviewed in details in [22]. The core concept of most of the islanding detection techniques remain the same that some of the system parameters (like voltage, frequency, etc.) change greatly with islanding but not much when the distribution system is grid connected. Islanding detection techniques can broadly be divided into remote and local techniques.

Remote islanding detection techniques are based on the communication between utilities and DGs. Supervisory Control and Data Acquisition (SCADA) [3] or power line signaling scheme [4]-[6] can be used to determine when the distribution system is islanded. These techniques have better reliability but they are expensive to implement especially for small systems. Therefore, local techniques are widely used to detect islanding and they can further be divided into passive and active techniques.

Passive methods continuously monitor the system parameters such as voltage, frequency, harmonic distortion, etc. Based on the system characteristics, one or more of these parameters may vary greatly when the system is islanded. Setting a proper threshold can help to differentiate between an islanding and a grid connected condition. Rate of change of output power of DG [3]-[7], rate of change of frequency [8], rate of change of frequency over power [9], change of source impedance [10],[11], voltage unbalance [12],[13], harmonic distortion [12],[14],[15] and frequency monitoring with reconfiguration of frequency relay [16] are a few examples of passive islanding detection techniques. A detection technique that looks into a database created by extensive off-line calculations is presented in [17] to overcome some of the limitations of existing passive techniques. The main problem with the passive detection techniques is that, it is difficult to detect islanding when the load and generation in the islanded system closely match. Furthermore, special care has to be taken while setting the thresholds for these parameters. If the threshold is too low, then it could result in nuisance tripping of DG and if the threshold is set too high, islanding may not be detected. The limitation of the passive detection techniques can be overcome by active techniques, which can detect islanding even under a perfect match of generation and load in the islanded system.

Active methods directly interact with the power system operation by introducing perturbations. These small perturbations will result in a significant change in system parameters when the DG is islanded, whereas the change will

be negligible when the DG is connected to the grid. Reactive power export error detection method [8], impedance measurement method [10], slip-mode frequency shift algorithm (SMS) [18], active frequency drift (AFD) [19], active frequency drift with positive feedback (AFDPF) [19], automatic phase-shift (APS) [20] and adaptive logic phase shift (ALPS) [21] are a few examples of active islanding detection techniques. The problems with these techniques are that they introduce perturbations in the system and detection time is slow as a result of extra time needed to analyze the system response of the perturbations. Furthermore, the perturbations are injected at predefined intervals even though it is unnecessary during most operating conditions. Also, if islanding occurs during an interval, then it has to wait for next perturbation to be applied before it can be detected, which further elongates the detection time. Applications of active techniques are limited to the DG type and/or load, i.e. reactive power export error detection method cannot be used when the DG has to operate at the unity power factor and methods based on phase shift are mostly useful for inverter based DGs. Also, AFD is very effective for purely resistive loads but it may fail for other loads [18]. Active methods based on impedance measurement introduce high frequency signals, AFD injects a distorted current waveform, and SMS, AFDPF, APS and ALPS shifts the phase of output current. This will often lower the quality of power. Therefore, there is a need to develop an efficient methodology to detect islanding of the distribution system with DG, without adverse effects to the system.

Most of the DGs around the world are required to operate at unity power factor. Hence, it is likely that there will be deficiency of reactive power once the distribution system is islanded. Capacitor banks may be the sole source of reactive power in the islanded distribution system with DG operating at unity power factor. The amount of reactive power they produce is a function of the voltage and once the voltage changes, as a result of islanding, the reactive power generated by the capacitor bank will also change, which will further change the voltage. This paper presents an integration of average rate of voltage change (passive method) and real power shift (active method), as a hybrid islanding detection technique to overcome the short comings of both active and passive techniques, to detect the islanding of a distribution system with DGs.

The proposed methodology is explained in detail in Section II and it is tested in a radial distribution system, which is presented in Section III. The methodology is simulated in DigSILENT PowerFactory 13.2.334. Different events have been simulated and the results are presented in Section IV. Section V concludes the paper.

II. PROPOSED METHODOLOGY

The flow chart of the proposed methodology is shown in Figure 1. Voltage is measured every period at one of the DG buses. After $dV/dt \neq 0$ is detected, the magnitude of average rate of voltage change for 5 periods, $Av5$, is used to determine

whether the system has been islanded or not. If $Av5$ is larger than a minimum set point, V_{SMin}, islanding is suspected. If it is larger than maximum set point, V_{SMax}, as a result of a large mismatch of generation and demand, it is clear that the distribution system is islanded. However, if $Av5$ is between V_{SMin} and V_{SMax}, then the change in voltage could be the result of an islanding or any other event in the system like switching, load change, etc. Then real power shift (RPS) is used.

The RPS will increase or decrease the real power generation of one of the DGs with increasing or decreasing voltage at the corresponding bus, respectively. The change of the real power generation of DG also satisfies the condition of DG operating at the unity power factor. Now, the magnitude of average rate of voltage change for 20 periods ($Av20$), after initiation of RPS, is used to differentiate islanding from any other event in the system. If $Av20$ is larger than V_{SMaxU} (set point to detect islanding with RPS), then it is from an islanding condition.
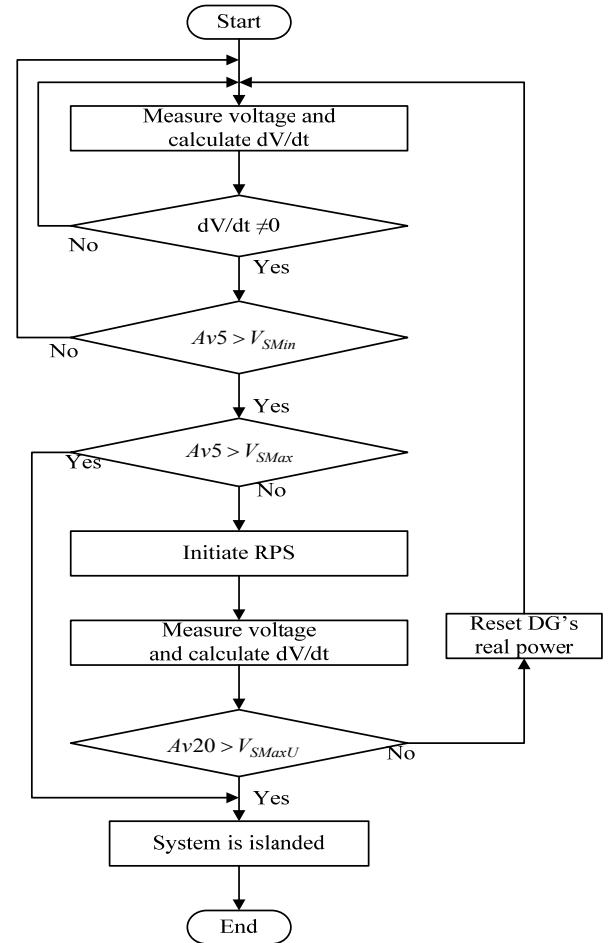

Fig. 1. Flow chart of the proposed methodology

In figure 1,
$$Av5 = \left| \frac{1}{5} \sum_{i=1}^{5} \left(\frac{dV_{DG}}{dt} \right)_i \right| \quad \text{(1)}$$

$$Av20 = \left| \frac{1}{20} \sum_{i=1}^{20} \left(\frac{dV_{DG}}{dt} \right)_i \right| \quad \text{(2)}$$
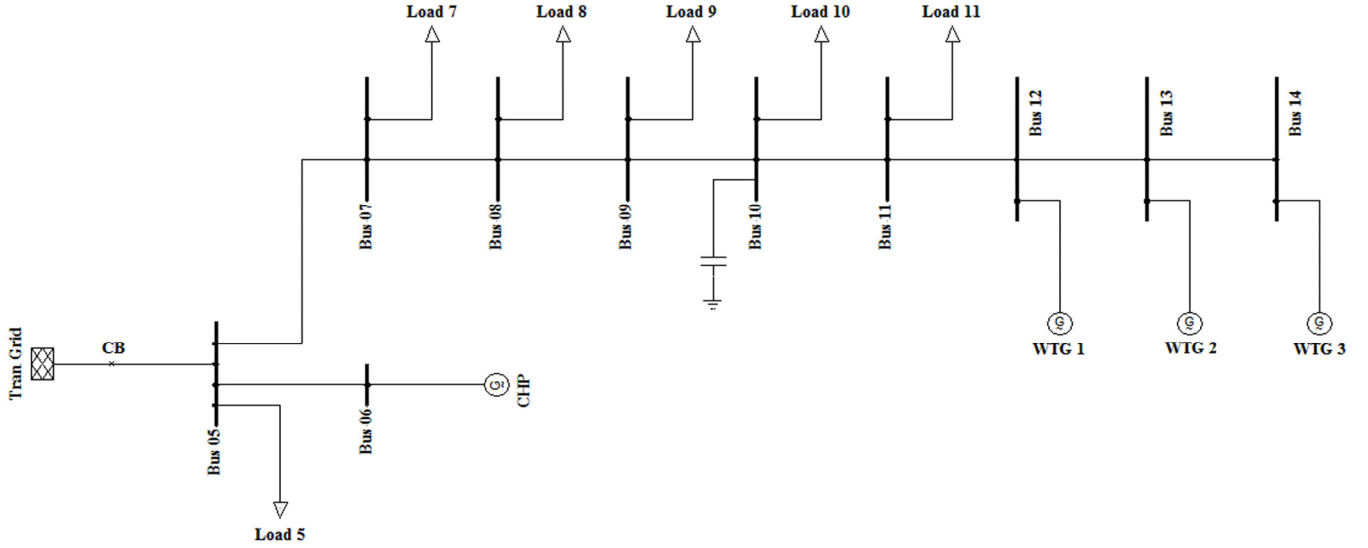
Fig. 2. Test system

Voltage measurement can be instantaneous and is done every cycle. $Av5$ is computed based upon the voltage measurement for the last 5 cycles that can be very fast with micro-controllers currently available in market. Hence, in case of large mismatch, islanding can be detected in almost 5 voltage cycles. In case of $V_{SMin} < Av5 < V_{SMax}$, the micro-controller sends a signal to initiate RPS and computes $Av20$ based on the voltage measurement of the next 20 cycles. Hence, islanding can be detected in around 25 voltage cycles even when the generation and load closely matches. The values for RPS, V_{SMin}, V_{SMaxU} and V_{SMax} are system specific and can be set accordingly. If high sensitivity is required, then V_{SMin} should be set smaller. RPS should be set at ramp rate rating of the DG. It is recommended that V_{SMax} should be set such that it is higher than $Av5$ achieved by 0.5 MW and 0.5 Mvar mismatch. V_{SMaxU} should be set corresponding to RPS such that it is more than $Av20$ achieved by islanding and RPS for a match of generation and demand. A look up table with $Av5$ for different power mismatch is given in Table AI. The table may be referred to set the values for V_{SMin}.

III. TEST SYSTEM

Figure 2 shows the test system in which the proposed methodology is tested. The test system is a part of a distribution network, owned by Himmerlands Elforsyning, in Aalborg, Denmark. The line data for the test system is given in Table AII. The test system consists of 6 loads, a capacitor bank, 3 fixed speed wind turbine generators (WTGs) and a CHP. Generator data is given in Table AIII. The distribution system is connected to the transmission network at Bus 05. The data for the transmission grid, represented as Tran Grid in Figure 2, is given in Table AIV. Islanding is simulated by opening the circuit breaker (CB). WTGs operate at the unity power factor and so does the CHP. The data for the base case load and generation is given in Table AV. Loads are modeled as in (3).

$$\left. \begin{aligned} P &= P_0(1 + K_{f_p}\Delta f + K_{v_p}\Delta V) \\ Q &= Q_0(1 + K_{f_q}\Delta f + K_{v_q}\Delta V) \end{aligned} \right\} \quad \textbf{(3)}$$

Where,

P and P_0 are active power at new voltage and frequency, and base voltage and frequency, respectively

Q and Q_0 are reactive power at new voltage and frequency, and base voltage and frequency, respectively

K_{f_p} and K_{v_p} are the coefficients of active load dependency on frequency and voltage, respectively

K_{f_q} and K_{v_q} are the coefficients of reactive load dependency on frequency and voltage, respectively

Δf and ΔV are the deviations on frequency and voltage, respectively.

Three different load models are simulated with $K_f (= K_{f_p} = K_{f_q}) = K_v (= K_{v_p} = K_{v_q}) = 0$ (load type 1), $K_f = K_v = 1$ (load type 2) and $K_f = K_v = 2$ (load type 3).

IV. SIMULATION RESULTS AND DISCUSSIONS

Various events (islanding, load change, capacitor switching, induction motor starting, short circuit and WTG switching) have been simulated to show the effectiveness of the proposed methodology. All these events are simulated at *time = 0 s*. The value for V_{SMin} is set at 11 V/s, as it is observed from the Table AI that islanding with the mismatch of as minimum as 1 kW and 1 kvar would result in $Av5 = 11$ V/s. V_{SMax} is set as 5000 V/s to be absolutely certain that this value is reached only for islanding and V_{SMaxU} is set at 100 V/s. CHP is chosen for RPS. RPS will change the CHP's real power at 4% per second (ramp rate rating of CHP generators). RPS is initiated at *time = 0.1 s*, if necessary. If initiated, at the ramp rate of 4% per second, RPS will gradually increase or

decrease CHP's real power by 1.6% by *0.5 s*, with increasing or decreasing voltage at CHP bus, respectively. Voltage measurement from 0.1 s to 0.5 s is used to calculate $Av20$ and RPS is deactivated if $Av20 < V_{SMaxU}$. Four different scenarios, with four different loading conditions, are considered.

A. Scenario I

Load 5, in this case, is 4.86 MW and 1.84 Mvar resulting in power deficiency of 0.7 MW and 0.7 Mvar in the islanded system. Figure 3 shows the CHP bus voltage for islanding. The magnitude of average rate of voltage change for the first five voltage cycles, $Av5$, = 8708.6 V/s, 7733.5 V/s and 6984.9 V/s, for load types 1, 2 and 3, respectively, which are all larger than V_{SMax}. Hence, islanding is detected without RPS as $Av5 > V_{SMin}$.
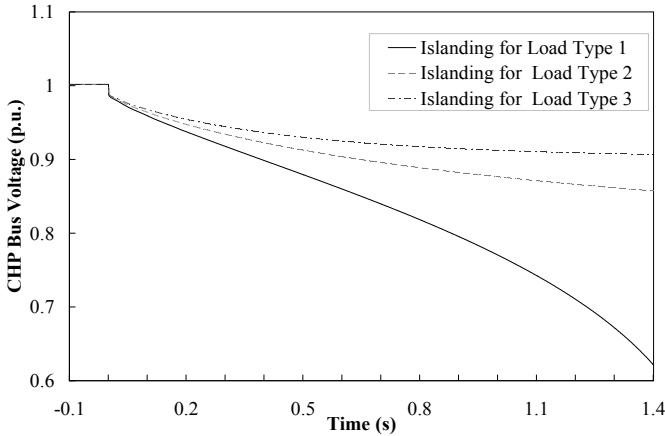

Fig. 3. CHP bus voltage for islanding
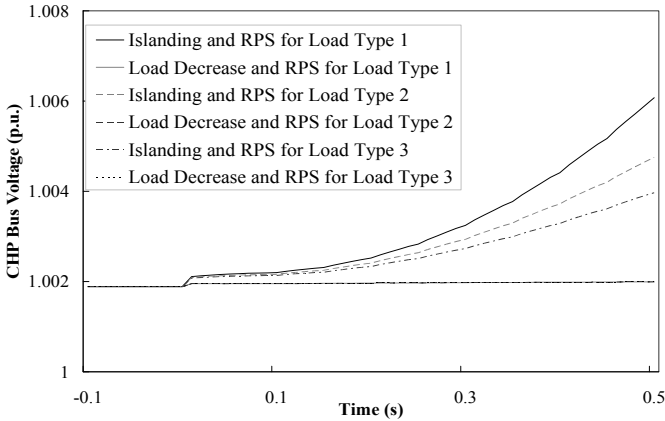
B. Scenario II

Fig. 4. CHP bus voltage for Load 5 decreasing by 50% and RPS compared to islanding and RPS

In this case, the real power demand at Bus 05 is 3.87 MW and the reactive power demand is 0.85 Mvar resulting in deficiency of 0.01 MW of real power and surplus of 0.01 Mvar of reactive power in the distribution system. Figures 4 and 5 show the change in CHP bus voltage for Load 5 decreasing by 50% and RPS, and 1.5 Mvar capacitor switching on at Bus 09 and RPS, respectively compared to

islanding and RPS. $Av5$ for islanding are 92.8 V/s, 82.9 V/s and 75.7 V/s for load types 1, 2 and 3, respectively. Similarly, $Av20$ for islanding, after RPS is initiated, are 192.96 V/s, 138.95 V/s and 101.25 V/s for load type 1, 2 and 3, respectively. This means that islanding is detected correctly as $Av20 > V_{SMaxU}$.

For the event with Load 5 decreasing by 50%, $Av5$ for all load types is 22.7 V/s, which is larger than V_{SMin} but smaller than V_{SMax}. So, RPS is initiated. Now, $Av20$ for all load types is 1.94 V/s, which is smaller than V_{SMaxU}. Hence, as the case should be, no islanding is detected by the routine.
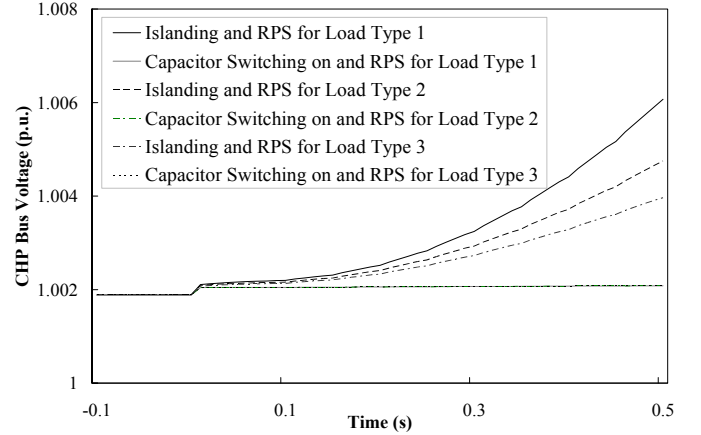
Fig. 5. CHP bus voltage for capacitor switching on and RPS compared to islanding and RPS

$Av5$, for capacitor switching on event, is 54.5 V/s for all load types. Again, values for $Av5$ is larger than V_{SMin} but smaller than V_{SMax}. RPS is initiated as a result of that. $Av20$ for all load types is 1.74 V/s, which is smaller than V_{SMaxU}. Hence, the algorithm ignores the event as any other event other than islanding.

C. Scenario III
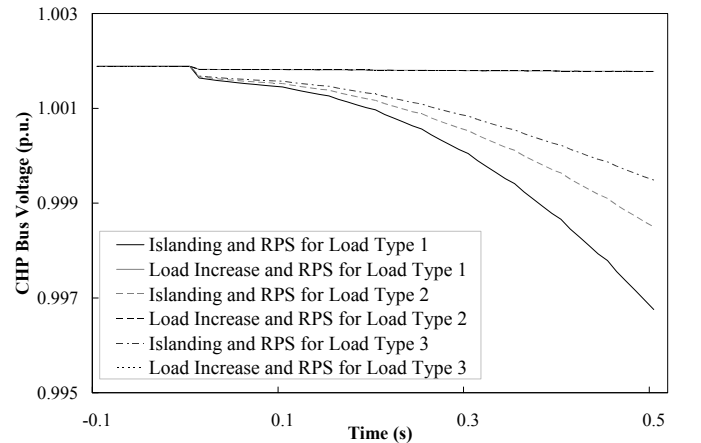
Fig. 6. CHP bus voltage for Load 5 increasing and RPS compared to islanding and RPS

In this case, the real power demand at Bus 05 is 3.87 MW and the reactive power demand is 0.87 Mvar, resulting in real and reactive power deficiency of 0.01 MW and 0.01 Mvar in

the distribution system, respectively. Figures 6-11 show the change in voltage at the CHP bus for Load 5 increasing by 50% and RPS, switching off the capacitor at Bus 10 and RPS, induction motor load of 0.5 MW starting at Bus 08 and RPS, a single phase to ground fault at Bus 12 and RPS, a three phase short circuit at Bus 12 and RPS, and wind turbine generator at Bus 12 (WTG1) switching off, respectively compared to islanding and RPS. $Av5$ for islanding are 118.8 V/s, 102.3 V/s and 90.4 V/s for load types 1, 2 and 3, respectively. Hence, RPS is initiated and $Av20$ for islanding are 233.83 V/s, 150.67 V/s and 103.82 V/s for load types 1, 2 and 3, respectively. Islanding is detected correctly as the values for $Av20$ for all load types are larger than V_{SMaxU}.

In case of Load 5 increasing by 50% event, $Av5$ for all load types is 23.0 V/s, which is larger than V_{SMin} but smaller than V_{SMax}. So, RPS is initiated. $Av20$ for all load types is 1.94 V/s, which is smaller than V_{SMaxU}. Hence, the algorithm ignores the event again as any other event other than islanding.

$Av5$, for capacitor switching off event, is 54.3V/s for all load types. RPS, initiated as a result of $V_{SMin} < Av5 < V_{SMax}$, results in $Av20 = 1.77$ V/s for all load types. $Av20$ is smaller than V_{SMaxU}. Hence, as should be the case, no islanding is detected again.
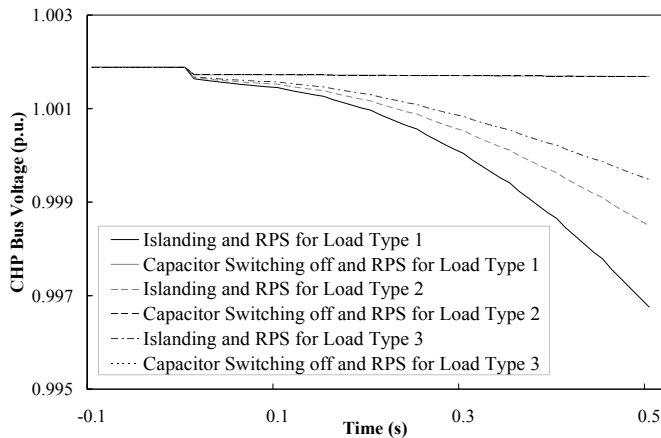

Fig. 7. CHP bus voltage for capacitor switching off and RPS compared to islanding and RPS

In case of a 0.5 MW induction motor starting at Bus 08 event, $Av5$ is 166.6 V/s for all load types. Again, values for $Av5$ is larger than V_{SMin} but smaller than V_{SMax}. RPS initiated as a result of that would result in $Av20$ of 1.97 V/s for all load types. $Av20$ is smaller than V_{SMaxU}. Hence, the algorithm correctly identifies the induction motor starting event as not islanding.

Distribution systems in Denmark use compensated grounding technique that permits sustained operation at single phase to ground faults. As the earth faults don't produce a significant fault current, clearing the fault takes longer time. In case of a single phase to ground fault at phase A of Bus 12, $Av5$ are 164.11 V/s, 163.91 V/s and 163.72V/s, respectively for type 1, 2 and 3 loads. RPS is initiated as a result of that. $Av20$ is 2.44 V/s for all load types. $Av5$ and $Av20$ are

calculated by measuring the voltage at the faulty phase. Hence, the algorithm doesn't detect islanding.
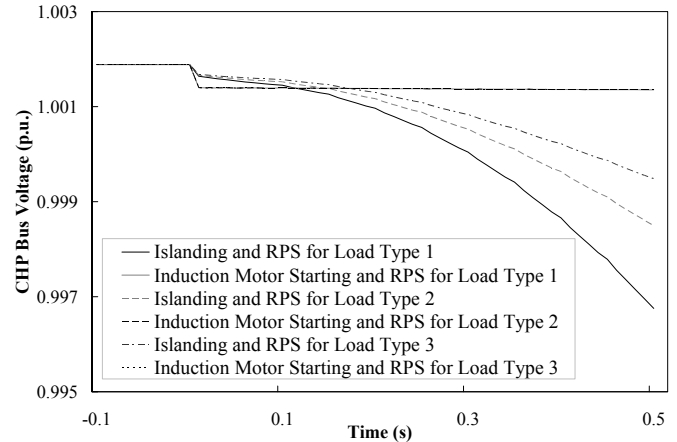
Fig. 8. CHP bus voltage for induction motor starting and RPS compared to islanding and RPS
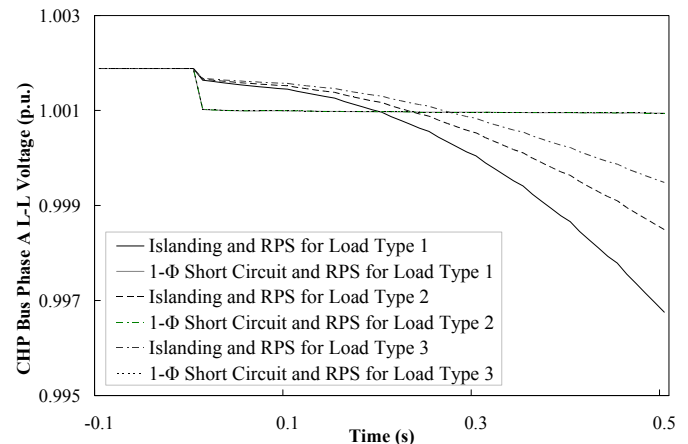
Fig. 9. CHP bus faulted phase line-line voltage for 1 phase to ground fault and RPS compared to islanding and RPS
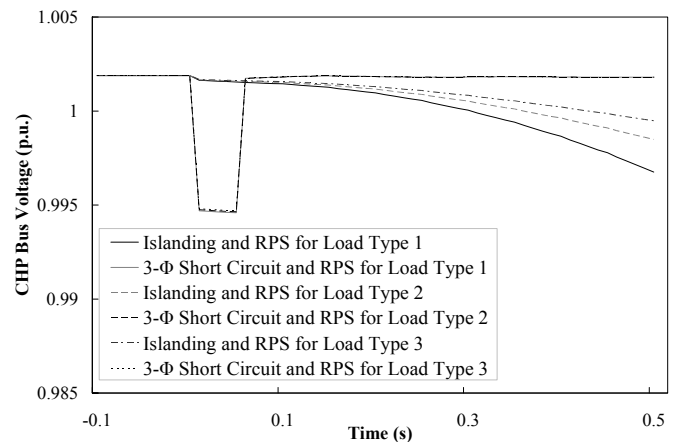
Fig. 10. CHP bus voltage for 3 phase short circuit and RPS compared to islanding and RPS

Fault current during the three phase short circuit is high and results in recloser operation. Reclosers operate in a sequence of two "fast" and two "time delayed" trip operations before locking out. The fast operation allows a recloser to trip for a

temporary fault downstream. The typical recloser opening time used in Danish distribution network during the fast operation is 500 ms. This means that during RPS, no recloser trip action occur which could give a large $Av20$. In figure 10, for a 3 phase short circuit at Bus 12, the recloser opens at *0.05 s* to clear the fault. $Av5$ is 102.53 V/s, 101.85 V/s and 101.21 V/s for type 1, 2 and 3 loads, respectively. RPS is initiated as a result of this. $Av20$ of 0.68 V/s is achieved for all load types. $Av20$ is smaller than V_{SMaxU} for all load types. Hence, islanding is not detected.

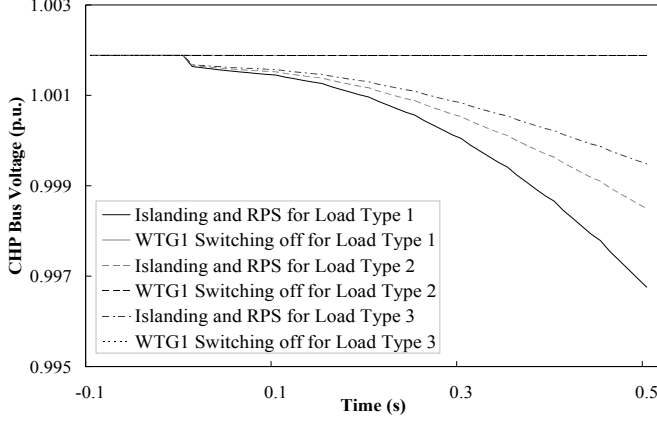Fig. 11. CHP bus voltage for WTG1 switching off compared to islanding and RPS

$Av5$ for WTG1 switching off event is 1.1 V/s. It is interesting to note that $Av5$ for this event is even smaller than V_{SMin}. RPS is not initiated ignoring the event as any other event other than islanding.
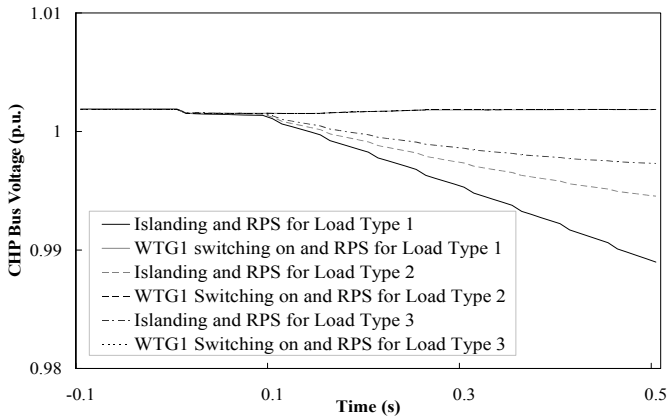
D. Scenario IV

Fig. 12. CHP bus voltage for WTG1 switching on and RPS compared to islanding and RPS

In this case, the real power demand at Bus 05 is 3.57 MW and the reactive power demand is 0.87 Mvar, resulting in real and reactive power deficiency of 0.01 Mw and 0.01 Mvar in the islanded system, respectively. The wind turbine generator at Bus 12 (WTG1) is disconnected. Figure 12 shows the CHP bus voltage for WTG1 switching on event and RPS, compared to islanding and RPS.

$Av5$ for WTG1 switching on event is 115 V/s for all load types. $Av5$ is larger than V_{SMin} but smaller than V_{SMax}. So, RPS is initiated. Now, $Av20$ for all load types is 15.62 V/s, which is smaller than V_{SMaxU}. Hence, islanding is not detected. $Av5$ for islanding, are 146.4 V/s, 126.6 V/s and 112.5 V/s for load types 1, 2 and 3, respectively. Similarly, $Av20$ for islanding are 241.9 V/s, 155.03 V/s and 106.45 V/s for load types 1, 2 and 3, respectively. Here, $Av20$ is larger than V_{SMaxU} resulting in islanding being detected. All the results are summarized in Table I.

TABLE I
RATE OF VOLTAGE CHANGE FOR DIFFERENT EVENTS

Events	AV 5 (V/s)			AV 20 (V/s)		
	Load Type			Load Type		
	1	2	3	1	2	3
Scenario I						
Islanding	8709	7734	6985	-	-	-
Scenario II						
Islanding	92.8	82.9	75.7	192.9	138.9	101.2
Load Decrease	22.7	22.7	22.7	1.94	1.94	1.94
Capacitor Switch On	54.5	54.5	54.5	1.74	1.74	1.74
Scenario III						
Islanding	118.8	102.3	90.4	233.8	150.7	103.8
Load Increase	23.0	23.0	23.0	1.94	1.94	1.94
Capacitor Switch Off	54.3	54.3	54.3	1.77	1.77	1.77
Induction Motor starting	166.6	166.6	166.6	197	1.97	1.97
1 phase to ground fault	164.1	163.9	163.1	15.1	15.1	15.1
3 phase short circuit	102.5	101.9	101.2	0.68	0.68	0.68
WTG Switching Off	1.1	1.1	1.1	-	-	-
Scenario IV						
Islanding	146.4	126.6	112.5	241.9	155.0	106.5
WTG Switching On	115.0	115.0	115.0	15.62	15.62	15.62

Results show that when there is a large mismatch in generation and demand, islanding can easily be detected by observing rate of voltage change. It is difficult to detect islanding when load and generation in the islanded distribution system closely match. Events like starting induction motor loads, short circuits or connecting wind turbines to grid can have average rate of voltage change which can be larger than the average rate of voltage change for islanding. Results also show that the RPS initiated after the suspicion of islanding results in higher $Av20$ when the system is actually islanded compared to other events in the system. In other words, RPS doesn't change the CHP bus voltage much when the distribution system is connected to the transmission grid, which supplies the deficient power or absorb the excess power in the distribution system. However, RPS initiated after the suspicion of islanding changes the CHP bus voltage significantly when the distribution system is islanded. Hence, the RPS can have absolute discrimination between islanding and other events even when the load and generation of islanded system closely match.

V. Conclusions

A hybrid technique has been proposed to detect islanding of a distribution system with multiple DG units operating at the unity power factor. It combines the real power shift and average rate of voltage change to efficiently detect islanding under various loading conditions.

The proposed technique uses RPS only when the passive technique (average rate of voltage change) cannot have a clear discrimination between grid connected and islanding condition. This eliminates the necessity of injecting disturbance from time to time to detect islanding like other active techniques. RPS only changes the real power of DG, which satisfies the condition of DG operating at the unity power factor. In the proposed technique, only one DG changes the real power in contrast to positive feedback techniques, where all the DGs work together to inject perturbation in the system. Also the proposed technique is able to efficiently discriminate islanding from various other events in the distribution system. Furthermore, islanding can be detected even when the load and the generation closely match. Even though, the method may fail to detect islanding for a perfect match of demand and generation in the islanded system, any subsequent change in load or generation in the islanded system will lead to change in voltage and the islanding being detected.

The proposed hybrid islanding detection technique, which combines the active and passive techniques, can efficiently detect islanding.

Appendix

TABLE AI
Look up table

Power Deficiency	$Av5$ (V/s)	Power Deficiency	$Av5$ (V/s)
0.1 kW + 0.1 kvar	1.54	5 kW + 5 kvar	55.09
0.5 kW + 0.5 kvar	5.89	10 kW + 10 kvar	118.80
1 kW + 1 kvar	11.00	20 kW + 20 kvar	219.75
2 kW + 2kvar	22.22	30 kW + 30 kvar	329.92
3 kW + 3 kvar	33.05	40 kW + 40 kvar	440.49
4 kW + 4 kvar	44.27	50 kW + 50 kvar	550.65

TABLE AII
Line data for the test system

From Bus	To Bus	Resistance (Ω)	Reactance (Ω)
5	6	0.1256	0.1404
5	7	0.1344	0.0632
7	8	0.1912	0.0897
8	9	0.4874	0.2284
9	10	0.1346	0.0906
10	11	1.4555	1.1130
11	12	0.6545	0.1634
12	13	0.0724	0.0181
13	14	0.7312	0.3114

TABLE AIII
Generators data

Parameters	CHP	WTG
Type of generator	Synchronous	Asynchronous
Number of Parallel Machine	3	1
Transformer to connect to grid	3.3 MVA 20/6.3 kV	630 kVA 20/0.4 kV
Individual generator's rating		
Rated Power	3.3 MW	630 kW
Rated Voltage	6.3 kV	0.4 kV
Stator resistance	0.0504 p.u.	0.018 p.u
Stator reactance	0.1 p.u.	0.015 p.u
Synchronous reactance d-axis	1.5 p.u.	
Synchronous reactance q-axis	0.75 p.u.	
Transient reactance d-axis	0.256 p.u.	
Sub-transient reactance d-axis	0.168 p.u.	
Sub-transient reactance q-axis	0.184 p.u.	
Transient time constant d-axis	0.53 s	
Sub-tran. time constant d-axis	0.03 s	
Sub-tran. time constant q-axis	0.03 s	
Mag. Reactance		4.42 p.u.
Rotor Resistance		0.0108 p.u.
Rotor Reactance		0.128 p.u.
Inertia Time Constant	0.54 s	0.38 s

TABLE AIV
Transmission system data

Parameters	Value
Maximum short circuit power	10000 MVA
Minimum short circuit power	8000 MVA
Maximum R/X ratio	0.1
Maximum Z2/Z1 ratio	1
Maximum X0/X1 ratio	1
Maximum R0/X0 ratio	0.1

TABLE AV
Load and generation data for the test system

Bus	PG (MW)	QG (Mvar)	PL (MW)	QL (Mvar)
05	0	0	3.87	0.85
06	6	0	0.0	0.0
07	0	0	0.56	0.11
08	0	0	0.56	0.11
09	0	0	0.55	0.10
10	0	1.5	0.85	0.20
11	0	0	0.51	0.13
12	0.31	0	0.0	0.0
13	0.31	0	0.0	0.0
14	0.31	0	0.0	0.0

REFERENCES

[1] *Recommended Practice for Utility Interconnected Photovoltaic (PV) Systems*, IEEE Standard 929-2000, 2000.

[2] *IEEE Standard for Interconnecting Distributed Resources into Electric Power Systems*, IEEE Standard 1547TM, June 2003.

[3] M. A. Refern, O. Usta, and G. Fielding, "Protection against loss of utility grid supply for a dispersed storage and generation unit," *IEEE Tran. Power Delivery*, vol. 8, no. 3, pp. 948-954, July 1993.

[4] M. Ropp, K. Aaker, J. Haigh, and N. Sabhah, "Using Power Line Carrier Communications to Prevent Islanding," i*n Proc. 28th IEEE Photovoltaic Specialist Conference*, pp. 1675-1678, 2000.

[5] W. Xu, G. Zhang, C. Li, W. Wang, G. Wang, and J. Kliber, "A power line signaling based technique for anti-islanding protection of distributed generators—part i: scheme and analysis," *IEEE Tran. Power Delivery*, vol. 22, no. 3, pp. 1758-1766, July 2007.

[6] G. Wang, J. Kliber, G. Zhang, W. Xu, B. Howell, and T. Palladino, "A power line signaling based technique for anti-islanding protection of distributed generators—part ii: field test results," *IEEE Tran. Power Delivery*, vol. 22, no. 3, pp. 1767-1772, July 2007.

[7] M. A. Redfern, J. I. Barren, and O. Usta, "A new microprocessor based islanding protection algorithm for dispersed storage and generation units," *IEEE Trans. Power Delivery*, vol. 10, no. 3, pp. 1249-1254, July 1995.

[8] J. Warin, and W. H. Allen, "Loss of mains protection," in *Proc. 1990 ERA Conference on Circuit Protection for industrial and Commercial Installation*, London, UK, pp. 4.3.1-12.

[9] F. Pai, and S. Huang, "A detection algorithm for islanding-prevention of dispersed consumer-owned storage and generating units," *IEEE Trans. Energy Conversion*, vol. 16, no. 4, pp. 346-351, 2001.

[10] P. O'Kane, and B. Fox, "Loss of mains detection for embedded generation by system impedance monitoring," in *Proc. Sixth International Conference on Developments in Power System Protection*, pp. 95-98, March 1997.

[11] P. D. Hopewell, N. Jenkins, and A. D. Cross, "Loss of mains detection for small generators," *IEE Proc. Electric Power Applications*, vol. 143, no. 3, pp. 225-230, May 1996.

[12] S. I. Jang, and K. H. Kim, "A new islanding detection algorithm for distributed generations interconnected with utility networks," in *Proc. IEE International Conference on Developments in Power System Protection*, vol.2, pp. 571-574, April 2004.

[13] S. I. Jang, and K. H. Kim, "An islanding detection method for distributed generations using voltage unbalance and total harmonic distortion of current," *IEEE Tran. Power Delivery*, vol. 19, no. 2, pp. 745-752, April 2004.

[14] S. Jang, and K. Kim, "Development of a logical rule-based islanding detection method for distributed resources," in *Proc. IEEE Power Engineering Society Winter Meeting*, vol. 2, pp. 800-806, 2002.

[15] H. Kabayashi, K. Takigawa, and E. Hashimato, "Method for preventing islanding phenomenon on utility grid with a number of small scale PV systems," *Second IEEE Photovoltaic Specialists Conference*, vol.1, pp. 695-700, 1991.

[16] R. Belhomme, M. Plamondon, H. Nakra, G. Desrosiers, and C. Gagnon, "Case study on the integration of a non-utility induction generator to the Hydro-Quebec distribution network", *IEEE Tran. Power Delivery*, vol. 10, no. 3, pp. 1677-1684, July 1995.

[17] K. El-Arroudi, G. Joos, I. Kamwa, and D. T. McGillis, "Intelligent-Based Approach to Islanding Detection in Distributed Generation," *IEEE Tran. Power Delivery*, vol. 22, no. 2, pp. 828 – 835, April 2007

[18] G. A. Smith, P. A. Onions, and D. G. Infield, "Predicting islanding operation of grid connected PV inverters," *IEE Proc. Electric Power Applications*, vol. 147, pp. 1-6, Jan. 2000.

[19] M. E. Ropp, M. Begovic, and A. Rohatgi, "Analysis and performance assessment of the active frequency drift method of islanding prevention," *IEEE Tran. Energy Conversion*, vol. 14, no 3, pp. 810-816, Sep. 1999.

[20] G. Hung, C. Chang, and C. Chen. "Automatic phase shift method for islanding detection of grid connected photovoltaic inverter," *IEEE Trans. Energy Conversion*, vol. 18, no. 1, pp. 169-173, Mar. 2003.

[21] J. Yin, L. Chang, and C. Diduch, "A new adaptive logic phase-shift algorithm for anti-islanding protections in inverter-based DG systems," *2005 IEEE Power Electronics Specialists Conference*, pp. 2482-2486, 2005.

[22] P. Mahat, Z. Chen, and B. Bak-Jensen, "Review of islanding detection methods for distributed generation," *in Proc. 3rd International Conference on Electric Utility Deregulation and Restructuring and Power Technologies*, pp. 2743 – 2748, 6-9 April 2008.

Pukar Mahat received B.Eng and M.Eng degree from Kathmandu University, Nepal and Asian Institute of Technology, Thailand, respectively.

He was Research Associate at Asian Institute of Technology, Thailand. Since 2007, he has been a PhD candidate at Institute of Energy Technology, Aalborg University, Denmark. Mr. Mahat's research interest includes Distributed Generation, Wind Power Generation and Distribution System Planning. He is a Certified Engineer in Nepal..

Zhe Chen (M'95, SM'98) received the B.Eng. and M.Sc. degrees from Northeast China Institute of Electric Power Engineering, Jilin City, China, and the Ph.D. degree from University of Durham, U.K.

He was a Lecturer and then a Senior Lecturer with De Montfort University, U.K. Since 2002, Dr. Chen has been a Research Professor and is now a Professor with the Institute of Energy Technology, Aalborg University, Denmark. He is the coordinator of Wind Power System Research program at the Institute of Energy Technology, Aalborg University. His research areas are power systems, power electronics and electric machines; and his main current research interests are wind energy and modern power systems. He has more than 170 publications in his technical field.

Dr Chen is an Associate Editor (Renewable Energy) of the IEEE Transactions on Power Electronics, Guest Editor of the IEEE Trans. on PE on Special Issue on Power Electronics for Wind Energy Conversion. He is a Member of the Institution of Engineering and Technology (London, U.K.), and a Chartered Engineer in the U.K

Birgitte Bak-Jensen (M'88) received her M.Sc. degree in Electrical Engineering in 1986 and a Ph.D. degree in "Modeling of High Voltage Components" in 1992, both degrees from Institute of Energy Technology, Aalborg University, Denmark.

From 1986-1988, she was with Electrolux Elmotor A/S, Aalborg, Denmark as an Electrical Design Engineer. She is an Associate Professor in the Institute of Energy Technology, Aalborg University, where she has worked since August 1988. Her fields of interest are modeling and diagnosis of electrical components, power quality and stability in power systems. During the last years, integration of dispersed generation to the network grid has become one of her main fields, where she has participated in many projects concerning wind turbines and their connection to the grid.